

From Theory to Reality: A Design Framework for Integrated Communication and Computing Receivers

Kuranage Roche Rayan Ranasinghe[✉], Kengo Ando[✉] and Giuseppe Thadeu Freitas de Abreu[✉]
School of Computer Science and Engineering, Constructor University, 28759 Bremen, Germany
 (kranasinghe,kando,gabreu)@constructor.university

Abstract—We propose a novel flexible and scalable framework to design integrated communication and computing (ICC) – a.k.a. over-the-air computing (AirComp) – receivers. To elaborate, while related literature so far has generally focused either on theoretical aspects of ICC or on the design of beamforming (BF) algorithms for AirComp, we propose a framework to design receivers capable of simultaneously detecting communication symbols and extracting the output of the AirComp operation, in a manner that can: a) be systematically generalized to any nomographic function, b) scaled to a massive number of user equipments (UEs) and edge devices (EDs), and c) support the multiple computation streams. For the sake of illustration, we demonstrate the proposed method under a setting consisting of the uplink from multiple single-antenna UEs/EDs simultaneously transmitting communication and computing signals to a single multiple-antenna base station (BS)/access point (AP). The receiver, which seeks to detect all communication symbols and minimize the distortion over the computing signals, requires that only a fraction of the transmit power be allocated to the latter, therefore coming close to the ideal (but unattainable) condition that computing is achieved “for free”, without taking resources from the communication system. The design leverages the Gaussian belief propagation (GaBP) framework relying only on element-wise scalar operations, which allows for its use in massive settings, as demonstrated by simulation results incorporating up to 200 antennas and 200 UEs/EDs. They also demonstrate the efficacy of the proposed method under all various loading conditions, with the performance of the scheme approaching fundamental limiting bounds in the under/fully loaded cases.

Index Terms—ICC, GaBP, Over-the-Air Computing, opportunistic and massive.

I. INTRODUCTION

The integration of functionalities such as sensing [1] and computing [2] into communications systems is expected to be the key differential between the sixth-generation (6G) [3] and the current generation of wireless systems [4]. However, while both sensing and computing are equally relevant in expanding the impact of wireless systems onto the modern way of living, it can be said that integrated sensing and communications (ISAC) has proven a somewhat easier task than over-the-air computing (AirComp), as indicated by related literature which offers a fast-growing number of transceiver design approaches for ISAC [5]–[12], while the focus of AirComp contributions has remained so far on theoretical analysis [13]–[17] and beamforming (BF) schemes [18]–[20].

In view of the above, this article proposes a novel Gaussian belief propagation (GaBP)-based [21]–[23] receiver design framework for integrated communication and computing (ICC) in which both data symbols and computing signals are detected in order to yield effective joint communication and computing functionalities¹.

To this end, we first formulate a system model in which the communication and computing signals are transmitted simultaneously by the user equipments (UEs) or edge devices (EDs), both of which are to be detected by the receiving base station (BS) or access point (AP). We then derive the relevant message passing rules to extract the separate data symbol and computing streams via the GaBP framework, which is initialized with a closed-form solution to an optimal combiner design problem with successive interference cancellation (SIC).

For the sake of illustration and simplicity of exposition, in this first article, the message passing rules are designed to extract the full set of individual elements of the computing signal, as opposed to traditional schemes which only estimate a specific nomographic function, as a step towards extracting the statistical prior on the aforementioned measurement data. It can be understood from the derivations, however, that the message-passing rules for any desired nomographic function, such as those listed in [24], can also be obtained provided that the corresponding prior distributions are derived, which is relegated to a follow-up work.

As a result of the strategy, the proposed framework can (in principle) be applied systematically to compute any nomographic function and even to support the simultaneous computing of multiple computation streams. In addition, as a consequence of the low complexity inherent to the GaBP framework, the method can be scaled to massive setups, as demonstrated by simulation results shown for a system with up to 200 antennas at the BS/AP and 200 UEs/EDs. As a bonus, simulation results also indicate that the approach is effective even if the power allocated to the computing signals is only a fraction of that allocated to communications symbols, bringing the overall method close to the ideal condition that computing is achieved “for free”, without exploiting resources from the communication system.

The remainder of the article can be summarized as follows. The system model is described in Section II. The proposed method is then introduced in Section III. Finally, the performance of both the communication and computing functionalities is evaluated in Section IV, in terms of bit error rate (BER) and mean-squared-error (MSE), respectively.

¹The integration of sensing into the ICC framework considered in this manuscript, which would yield a more complete integrated sensing, communications and computing (ISCC) problem, is rather trivial under the assumption that the communication waveforms can be used for sensing purposes via their reflected echoes, as demonstrated by related literature [5]–[12]. However, due to space limitations, we leave the sensing component to be addressed directly in a follow-up work.

Notation: The following notation is used persistently throughout the manuscript. Vectors and matrices are represented by lowercase and uppercase boldface letters, respectively; \mathbf{I}_M denotes an identity matrix of size M and $\mathbf{1}_M$ denotes a column vector composed of M ones; the vector norm and the absolute value of a scalar are respectively given by $\|\cdot\|$ and $|\cdot|$; the transpose and hermitian operations follow the conventional form $(\cdot)^T$ and $(\cdot)^H$, respectively; $\Re\{\cdot\}$, $\Im\{\cdot\}$ and $\min(\cdot)$ represents the real part, imaginary part and the minimum operator, respectively. Finally, $\sim \mathcal{N}(\mu, \sigma^2)$ and $\sim \mathcal{CN}(\mu, \sigma^2)$ respectively denotes the Gaussian and complex Gaussian distribution with mean μ and variance σ^2 , where \sim stands for “is distributed as”.

II. SYSTEM MODEL

We consider an uplink multi-user single-input multiple-output (SIMO) system composed of K single-antenna UEs/EDs and one BS/AP equipped with N antennas, as illustrated in Fig. 1. Under the assumption of perfect symbol synchronization amongst users, the received signal $\mathbf{y} \in \mathbb{C}^{N \times 1}$ at the BS/AP subjected to fading and noise is given by

$$\mathbf{y} = \sum_{k=1}^K \mathbf{h}_k x_k + \mathbf{w}, \quad (1)$$

where the $\mathbf{h}_k \in \mathbb{C}^{N \times 1}$ denotes the channel vector between the k -th user and the BS/AP with each element $h_{n,k} \sim \mathcal{CN}(0, \sigma_h^2)$; $x_k \in \mathbb{C}$ is a concatenated transmit signal from k -th user and $\mathbf{w} \in \mathbb{C}^{N \times 1} \sim \mathcal{CN}(0, \sigma_w^2 \mathbf{I}_N)$ represents the additive white Gaussian noise (AWGN).

For the incorporation of both communication and computing functionalities into the system, the transmit signal can be decomposed and defined as a sum of its communication and computing parts, respectively, as

$$x_k \triangleq d_k + \psi_k(s_k), \quad (2)$$

where $d_k \in \mathcal{D}$ and $s_k \in \mathbb{R}^2$ denote k -th user's modulated symbol for communication and computing, respectively, with \mathcal{D} representing an arbitrary discrete constellation (e.g. quadrature amplitude modulation (QAM)) with cardinality D ; while $\psi_k(\cdot)$ denotes the pre-processing function for AirComp.

Adhering to the computing aspect which requires the computation of an AirComp target function at the BS/AP, we define $f(\mathbf{s})$ which can be described as

$$f(\mathbf{s}) = \phi \left(\sum_{k=1}^K \psi_k(s_k) \right) \rightarrow \sum_{k=1}^K s_k, \quad (3)$$

where ϕ represents the post-processing function for a general nomographic expression. For the sake of simplicity, the arithmetic sum operation is chosen in this manuscript for the target function $f(\mathbf{s})$.

²While the computing aspects usually incorporate the computation of a nomographic function composed of real variables [14], the extension to complex variables is trivial and holds for all the consequent derivations in the manuscript.

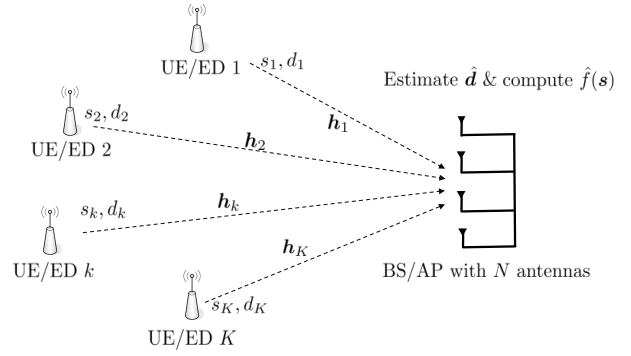


Fig. 1. Illustration of a SIMO ICC system consisting of one BS/AP with N antennas and K single antenna UEs/EDs.

For later convenience, the received signal can now be reformulated in terms of matrix operations as

$$\mathbf{y} = \mathbf{H}\mathbf{x} + \mathbf{w} = \mathbf{H}(\mathbf{d} + \mathbf{s}^\psi) + \mathbf{w}, \quad (4)$$

where the complex channel matrix $\mathbf{H} \triangleq [\mathbf{h}_1, \dots, \mathbf{h}_K] \in \mathbb{C}^{N \times K}$, the concatenated transmit signal $\mathbf{x} \triangleq [x_1, \dots, x_K]^T \in \mathbb{C}^{K \times 1}$, the data signal vector $\mathbf{d} \triangleq [d_1, \dots, d_K]^T \in \mathbb{C}^{K \times 1}$ and the computing signal vector $\mathbf{s}^\psi \triangleq [\psi_1(s_1), \dots, \psi_K(s_K)]^T \in \mathbb{R}^{K \times 1}$ are explicitly defined.

III. PROPOSED INTEGRATED COMMUNICATIONS AND COMPUTING RECEIVER DESIGN FRAMEWORK

In this section, we consider a joint data and computing signal detection scheme termed ICC using the well known GaBP algorithm. Without loss of generality (w.l.g.), the modulation for communications is assumed to be quadrature phase-shift keying (QPSK) and the k -th user's signal for computing is assumed to follow $s_k \sim \mathcal{N}(\mu_s, \sigma_s^2)$.

Since the goal of AirComp is to estimate a certain function that depends on the computing signal \mathbf{s} , the assumption that the mean of the elements μ_s is known is restrictive, motivating the development of a closed form initialization which is elaborated on in the latter sections.

A. Joint Detection and Computing

We now consider the joint estimation of the data symbols and the computing signals to fully recover the estimated data vector $\hat{\mathbf{d}} \in \mathbb{C}^{K \times 1}$ and the nomographic function $\hat{f}(\mathbf{s}) \in \mathbb{R}$ via the GaBP technique. As a consequence of the general element-wise structure of the GaBP, we can formulate a bivariate set of message passing rules where the data signal vector \mathbf{d} and the computing signal vector \mathbf{s} can be estimated separately, each with their own Bayes-optimal denoisers for the best decoding/computing performance.

To that end, in order to derive the scalar GaBP rules, let us first express equation (4) in an element-wise manner, dropping the superscript ψ for convenience, as

$$y_n = \sum_{k=1}^K h_{n,k} \cdot d_k + \sum_{k=1}^K h_{n,k} \cdot s_k + w_n. \quad (5)$$

Next, consider the i -th iteration of the algorithm, and denote the soft replicas of the k -th communication and computing

symbol with the n -th receive signal y_n at the previous iteration respectively by $\hat{d}_{n,k}^{(i-1)}$ and $\hat{s}_{n,k}^{(i-1)}$.

Then, the MSEs of these estimates computed for the i -th iteration are given by

$$\hat{\sigma}_{d:n,k}^{2(i)} \triangleq \mathbb{E}_d [|d - \hat{d}_{n,k}^{(i-1)}|^2] = E_D - |\hat{d}_{n,k}^{(i-1)}|^2, \forall(n, k), \quad (6a)$$

$$\hat{\sigma}_{s:n,k}^{2(i)} \triangleq \mathbb{E}_s [|s - \hat{s}_{n,k}^{(i-1)}|^2], \forall(n, k), \quad (6b)$$

where \mathbb{E}_d and \mathbb{E}_s respectively refers to expectation over all the possible symbols in the constellation \mathcal{D} and the expectation over all the possible outcomes of $s \sim \mathcal{N}(\mu_s, \sigma_s^2)$ with E_D explicitly denoting the data constellation power.

1) Soft Interference Cancellation: The objective of the soft interference cancellation (soft IC) stage at a given i -th iteration of the algorithm is to utilize the soft replicas $\hat{d}_{n,k}^{(i-1)}$ and $\hat{s}_{n,k}^{(i-1)}$ from a previous iteration to calculate the data- and computing-centric soft IC symbols $\tilde{y}_{d:n,k}^{(i)}$ and $\tilde{y}_{s:n,k}^{(i)}$ with their corresponding variances $\tilde{\sigma}_{d:n,k}^{2(i)}$ and $\tilde{\sigma}_{s:n,k}^{2(i)}$.

Therefore, exploiting equation (5), the soft IC symbols for both the data and computing signals are given as

$$\begin{aligned} \tilde{y}_{d:n,k}^{(i)} &= y_n - \sum_{q \neq k} h_{n,q} \hat{d}_{n,q}^{(i)} - \sum_{k=1}^K h_{n,k} \hat{s}_{n,k}^{(i)}, \\ &= h_{n,k} d_k + \underbrace{\sum_{q \neq k} h_{n,q} (d_q - \hat{d}_{n,q}^{(i)}) + \sum_{k=1}^K h_{n,k} (s_k - \hat{s}_{n,k}^{(i)})}_{\text{interference + noise term}} + w_n, \end{aligned} \quad (7a)$$

$$\begin{aligned} \tilde{y}_{s:n,k}^{(i)} &= y_n - \sum_{q \neq k} h_{n,q} \hat{s}_{n,q}^{(i)} - \sum_{k=1}^K h_{n,k} \hat{d}_{n,k}^{(i)}, \\ &= h_{n,k} s_k + \underbrace{\sum_{q \neq k} h_{n,q} (s_q - \hat{s}_{n,q}^{(i)}) + \sum_{k=1}^K h_{n,k} (d_k - \hat{d}_{n,k}^{(i)})}_{\text{interference + noise term}} + w_n, \end{aligned} \quad (7b)$$

In turn, leveraging scalar Gaussian approximation (SGA) to approximate the interference and noise terms as Gaussian noise, the conditional probability density functions (PDFs) of the soft IC symbols are given by

$$p_{\tilde{y}_{d:n,k}^{(i)} | d_k}(\tilde{y}_{d:n,k}^{(i)} | d_k) \propto \exp \left[-\frac{|\tilde{y}_{d:n,k}^{(i)} - h_{n,k} d_k|^2}{\tilde{\sigma}_{d:n,k}^{2(i)}} \right], \quad (8a)$$

$$p_{\tilde{y}_{s:n,k}^{(i)} | s_k}(\tilde{y}_{s:n,k}^{(i)} | s_k) \propto \exp \left[-\frac{|\tilde{y}_{s:n,k}^{(i)} - h_{n,k} s_k|^2}{\tilde{\sigma}_{s:n,k}^{2(i)}} \right], \quad (8b)$$

with their conditional variances expressed as

$$\tilde{\sigma}_{d:n,k}^{2(i)} = \sum_{q \neq k} |h_{n,q}|^2 \hat{\sigma}_{d:n,q}^{2(i)} + \sum_{k=1}^K |h_{n,k}|^2 \hat{\sigma}_{s:n,k}^{2(i)} + \sigma_w^2, \quad (9a)$$

$$\tilde{\sigma}_{s:n,k}^{2(i)} = \sum_{q \neq k} |h_{n,q}|^2 \hat{\sigma}_{s:n,q}^{2(i)} + \sum_{k=1}^K |h_{n,k}|^2 \hat{\sigma}_{d:n,k}^{2(i)} + \sigma_w^2. \quad (9b)$$

2) Belief Generation: With the goal of generating the beliefs for all the data and computing symbols, we first exploit SGA under the assumption that N is a sufficiently large number and that the individual estimation errors in $\hat{d}_{n,k}^{(i-1)}$ and $\hat{s}_{n,k}^{(i-1)}$ are independent.

Therefore, as a consequence of SGA and in hand of the conditional PDFs, the extrinsic PDFs are obtained as

$$\prod_{q \neq n} p_{\tilde{y}_{d:q,k}^{(i)} | d_k}(\tilde{y}_{d:q,k}^{(i)} | d_k) \propto \exp \left[-\frac{(d_k - \bar{d}_{n,k}^{(i)})^2}{\bar{\sigma}_{d:n,k}^{2(i)}} \right], \quad (10a)$$

$$\prod_{q \neq n} p_{\tilde{y}_{s:q,k}^{(i)} | s_k}(\tilde{y}_{s:q,k}^{(i)} | s_k) \propto \exp \left[-\frac{(s_k - \bar{s}_{n,k}^{(i)})^2}{\bar{\sigma}_{s:n,k}^{2(i)}} \right], \quad (10b)$$

where the corresponding extrinsic means are defined as

$$\bar{d}_{n,k}^{(i)} = \bar{\sigma}_{d:n,k}^{(i)} \sum_{q \neq n} \frac{h_{q,k}^* \cdot \tilde{y}_{d:q,k}^{(i)}}{\bar{\sigma}_{d:q,k}^{2(i)}}, \quad (11a)$$

$$\bar{s}_{n,k}^{(i)} = \bar{\sigma}_{s:n,k}^{(i)} \sum_{q \neq n} \frac{h_{q,k}^* \cdot \tilde{y}_{s:q,k}^{(i)}}{\bar{\sigma}_{s:q,k}^{2(i)}}, \quad (11b)$$

with the extrinsic variances given by

$$\bar{\sigma}_{d:n,k}^{2(i)} = \left(\sum_{q \neq n} \frac{|h_{q,k}|^2}{\bar{\sigma}_{d:q,k}^{2(i)}} \right)^{-1}, \quad (12a)$$

$$\bar{\sigma}_{s:n,k}^{2(i)} = \left(\sum_{q \neq n} \frac{|h_{q,k}|^2}{\bar{\sigma}_{s:q,k}^{2(i)}} \right)^{-1}. \quad (12b)$$

3) Soft Replica Generation: This stage involves the exploitation of the previously computed beliefs and denoising them via a Bayes-optimal denoiser to get the final estimates for the intended variables. A damping procedure can also be incorporated here to prevent convergence to local minima due to incorrect hard-decision replicas.

Since the data symbols originate from a discrete QPSK alphabet, w.l.g., the Bayes-optimal denoiser is given as

$$\hat{d}_{n,k}^{(i)} = c_d \cdot \left(\tanh \left[2c_d \frac{\Re\{\bar{d}_{n,k}^{(i)}\}}{\bar{\sigma}_{d:n,k}^{2(i)}} \right] + j \tanh \left[2c_d \frac{\Im\{\bar{d}_{n,k}^{(i)}\}}{\bar{\sigma}_{d:n,k}^{2(i)}} \right] \right), \quad (13)$$

where $c_d \triangleq \sqrt{E_D/2}$ denotes the magnitude of the real and imaginary parts of the explicitly chosen QPSK symbols, with its corresponding variance updated as in equation (6a).

Similarly, since the computing signal follows a Gaussian distribution, the denoiser with a Gaussian prior and its corresponding variance is given as ³

$$\hat{s}_{n,k}^{(i)} = \frac{\sigma_s^2 \cdot \bar{s}_{n,k}^{(i)} + \bar{\sigma}_{s:n,k}^{2(i)} \cdot \mu_s}{\bar{\sigma}_{s:n,k}^{2(i)} + \sigma_s^2}, \quad (14a)$$

³It is worth noting that if the post-processed computing signals have zero mean, the Gaussian denoiser will no longer require a closed-form initialization; i.e. the last three lines under the initialization section in Algorithm 1 can be ignored.

$$\hat{\sigma}_{s:n,k}^{2(i)} = \frac{\sigma_s^2 \cdot \bar{\sigma}_{s:n,k}^{2(i)}}{\bar{\sigma}_{s:n,k}^{2(i)} + \sigma_s^2}. \quad (14b)$$

After obtaining $\hat{d}_{n,k}^{(i)}$ and $\hat{s}_{n,k}^{(i)}$ as per equations (13) and (14a), the final outputs are computed by damping the results with damping factors $0 < \beta_d, \beta_s < 1$ in order to improve convergence [25], yielding

$$\hat{d}_{n,k}^{(i)} = \beta_d \hat{d}_{n,k}^{(i-1)} + (1 - \beta_d) \hat{d}_{n,k}^{(i-1)}, \quad (15a)$$

$$\hat{s}_{n,k}^{(i)} = \beta_s \hat{s}_{n,k}^{(i-1)} + (1 - \beta_s) \hat{s}_{n,k}^{(i-1)}. \quad (15b)$$

In turn, the corresponding variances $\hat{\sigma}_{d:n,k}^{2(i)}$ and $\hat{\sigma}_{s:n,k}^{2(i)}$ are first correspondingly updated via equations (6a) and (14b), respectively, and then damped via

$$\hat{\sigma}_{d:n,k}^{2(i)} = \beta_d \hat{\sigma}_{d:n,k}^{2(i-1)} + (1 - \beta_d) \hat{\sigma}_{d:n,k}^{2(i-1)}, \quad (16a)$$

$$\hat{\sigma}_{s:n,k}^{2(i)} = \beta_s \hat{\sigma}_{s:n,k}^{2(i-1)} + (1 - \beta_s) \hat{\sigma}_{s:n,k}^{2(i-1)}. \quad (16b)$$

Finally, as a result of the conflicting dimensions, the consensus update can be obtained as

$$\hat{d}_k = \left(\sum_{n=1}^N \frac{|h_{n,k}|^2}{\bar{\sigma}_{d:n,k}^{2(i)}} \right)^{-1} \left(\sum_{n=1}^N \frac{h_{n,k}^* \cdot \tilde{y}_{d:n,k}^{(i)}}{\bar{\sigma}_{d:n,k}^{2(i)}} \right), \quad (17a)$$

$$\hat{s}_k = \Re \left\{ \left(\sum_{n=1}^N \frac{|h_{n,k}|^2}{\bar{\sigma}_{s:n,k}^{2(i)}} \right)^{-1} \left(\sum_{n=1}^N \frac{h_{n,k}^* \cdot \tilde{y}_{s:n,k}^{(i)}}{\bar{\sigma}_{s:n,k}^{2(i)}} \right) \right\}, \quad (17b)$$

where we take advantage of the fact that \mathbf{s} is real.

B. Closed-form Initialization

For the computation of a target function $\sum s_k$ at the BS/AP, let us first reformulate the combining of the residual signal at the i -th iteration of the algorithm leveraging equation (4) after SIC of the estimated communication signal $\hat{\mathbf{d}}^{(i)}$ as

$$\tilde{f}^{(i)}(\mathbf{s}) = \mathbf{u}^H (\mathbf{y} - \mathbf{H} \hat{\mathbf{d}}^{(i)}) = \mathbf{u}^H (\mathbf{H}(\mathbf{s} - \tilde{\mathbf{d}}^{(i)}) + \mathbf{w}), \quad (18)$$

where $\mathbf{u} \in \mathbb{C}^{N \times 1}$ denotes the combining vector, and we intrinsically define a data signal error vector⁴ $\tilde{\mathbf{d}}^{(i)} \triangleq \hat{\mathbf{d}}^{(i)} - \mathbf{d} \in \mathbb{C}^{K \times 1}$.

Leveraging the above formulation, let us consider the optimization problem given by

$$\underset{\mathbf{u} \in \mathbb{C}^{N \times 1}}{\text{minimize}} \quad \|\mathbf{f}(\mathbf{s}) - \tilde{f}^{(i)}(\mathbf{s})\|_2^2, \quad (19)$$

where the objective function is defined as

$$\|\mathbf{f}(\mathbf{s}) - \tilde{f}^{(i)}(\mathbf{s})\|_2^2 \triangleq \|\mathbf{1}_K^T \cdot \mathbf{s} - \mathbf{u}^H (\mathbf{H}(\mathbf{s} - \tilde{\mathbf{d}}^{(i)}) + \mathbf{w})\|_2^2. \quad (20)$$

Then, the closed-form solution at a given i -th iteration for the combining vector can be derived as

$$\mathbf{u}^{(i)} = (\mathbf{H}(\sigma_s^2 \mathbf{I}_K + \mathbf{\Omega}^{(i)}) \mathbf{H}^H + \sigma_w^2 \mathbf{I}_N)^{-1} \cdot \mathbf{H}(\sigma_s^2 \mathbf{I}_K) \mathbf{1}_K, \quad (21)$$

where $\mathbf{\Omega}^{(i)} \triangleq \mathbb{E}[\tilde{\mathbf{d}} \tilde{\mathbf{d}}^H]$ is the instantaneous variance of the data signal computed via the GaBP.

C. Joint Integrated Communication and Computing Design

We now combine the low complexity GaBP with the AirComp initialization to estimate both the data signal $\hat{\mathbf{d}}$ and computing function $\hat{f}(\mathbf{s})$. The complete pseudocode for the procedure is summarized in Algorithm 1.

⁴ $\tilde{\mathbf{d}}^{(i)}$ is equivalent to the MSE of the data signal vector $\hat{\sigma}_{d:n,k}^{2(i)}$ averaged over all n to satisfy the conflicting dimensions.

Algorithm 1 Joint Data Detection & AirComp for Integrated Communication and Computing Systems

Input: receive signal vector $\mathbf{y} \in \mathbb{C}^{N \times 1}$, complex channel matrix $\mathbf{H} \in \mathbb{C}^{N \times K}$, maximum number of iterations i_{\max} , data constellation power E_D , noise variance σ_w^2 , computing signal variance σ_s^2 and damping factors β_d, β_s .

Output: $\hat{\mathbf{d}}$ and $\hat{f}(\mathbf{s})$

Initialization

- Set iteration counter to $i = 0$ and amplitudes $c_d = \sqrt{E_D/2}$.
 - Set initial data estimates to $\hat{d}_{n,k}^{(0)} = 0$ and corresponding variances to $\hat{\sigma}_{d:n,k}^{2(0)} = E_D, \forall n, k$.
 - Set initial computing signal estimates to $\hat{s}_{n,k}^{(0)} = 0$ and corresponding variances to $\hat{\sigma}_{s:n,k}^{2(0)} = \sigma_s^2, \forall n, k$.
 - Initialize $\mathbf{u}^{(0)}$ from equation (21).
 - Compute $\tilde{f}^{(i)}(\mathbf{s})$ from equation (18).
 - Set $\mu_s^{(0)} = \tilde{f}^{(i)}(\mathbf{s})/K$.
-

for $i = 1$ to i_{\max} **do**

Communication and Computing Update: $\forall n, k$

- 1: Compute soft IC data signal $\tilde{y}_{d:n,k}^{(i)}$ and its corresponding variance $\tilde{\sigma}_{d:n,k}^{2(i)}$ from equations (7a) and (9a).
 - 2: Compute soft IC computing signal $\tilde{y}_{s:n,k}^{(i)}$ and its corresponding variance $\tilde{\sigma}_{s:n,k}^{2(i)}$ from equations (7b) and (9b).
 - 3: Compute extrinsic data signal belief $\bar{d}_{n,k}^{(i)}$ and its corresponding variance $\bar{\sigma}_{d:n,k}^{2(i)}$ from equations (11a) and (12a).
 - 4: Compute extrinsic computing signal belief $\bar{s}_{n,k}^{(i)}$ and its corresponding variance $\bar{\sigma}_{s:n,k}^{2(i)}$ from eqs. (11b) and (12b).
 - 5: Compute denoised and damped data signal estimate $\hat{d}_{n,k}^{(i)}$ from equations (13) and (15a).
 - 6: Compute denoised and damped data signal variance $\hat{\sigma}_{d:n,k}^{2(i)}$ from equations (6a) and (16a).
 - 7: Compute denoised and damped computing signal estimate $\hat{s}_{n,k}^{(i)}$ from equations (14a) and (15b).
 - 8: Compute denoised and damped computing signal variance $\hat{\sigma}_{s:n,k}^{2(i)}$ from equations (14b) and (16b).
- Optional High Performance Update:**
- 9: Update $\mathbf{u}^{(i)}$ from equation (21).
 - 10: Update $\tilde{f}^{(i)}(\mathbf{s})$ from equation (18).
 - 11: Update $\mu_s^{(i)} = \tilde{f}^{(i)}(\mathbf{s})/K$.

end for

- 12: Calculate $\hat{d}_k, \forall k$ using equation (17a).
 - 13: Calculate $\hat{s}_k, \forall k$ using equation (17b).
 - 14: Compute $\hat{f}(\mathbf{s}) = \sum_{k=1}^K \hat{s}_k$.
-

IV. PERFORMANCE ASSESSMENT

For all the numerical simulations carried out, the total transmit power is held constant at 1 with 99% of the power allocated to the data signal and 1% of the power allocated to the computing signal. In addition, the computing signal is assumed to follow $s_k \sim \mathcal{N}(0, \sigma_s^2)$ and the channel coefficients follow $h_{n,k} \sim \mathcal{CN}(0, 1)$. Similarly, the algorithmic parameters are set as $\beta_d = 0.5$, $\beta_s = 0.8$ and $i_{\max} = 30$.

A. Numerical Results

For the numerical evaluation of our proposed method, we first consider a typical uplink system composed of a BS/AP with $N = 10$ antennas servicing a varying number of single-antenna users that are categorized into the underloaded, fully loaded and overloaded scenarios with $K = 2$, $K = 5$ and $K = 10$ users, respectively⁵.

Consequently, Fig. 2 now showcases BER and MSE results for the estimation of $\hat{\mathbf{d}}$ and $\hat{f}(s)$, respectively, for all three aforementioned cases as follows: the linear bound is obtained by running the proposed algorithm including the high performance update under the assumption that one of the estimates is perfectly known (*i.e.*, for the case of data detection, the computing signals are assumed to be known and vice-versa); the high performance result is computed by running the proposed algorithm with the high performance update included; the low complexity result is obtained by skipping the high performance update (*i.e.*, lines 9 – 11 in algorithm 1 are not executed) and finally, as a consequence of $s_k \sim \mathcal{N}(0, \sigma_s^2)$, the red dashed line presents the results when the closed-form initialization is also ignored.

As demonstrated by the results, we see that all the variations, with more emphasis on the fully and underloaded cases of the proposed algorithm approaches the linear bound in terms of BER with a slightly higher BER seen by the high performance result. In addition, although the fully and overloaded scenarios experience an error floor for the BERs at higher signal-to-noise ratios (SNRs), these effects can be overcome with larger system sizes as seen from our next result

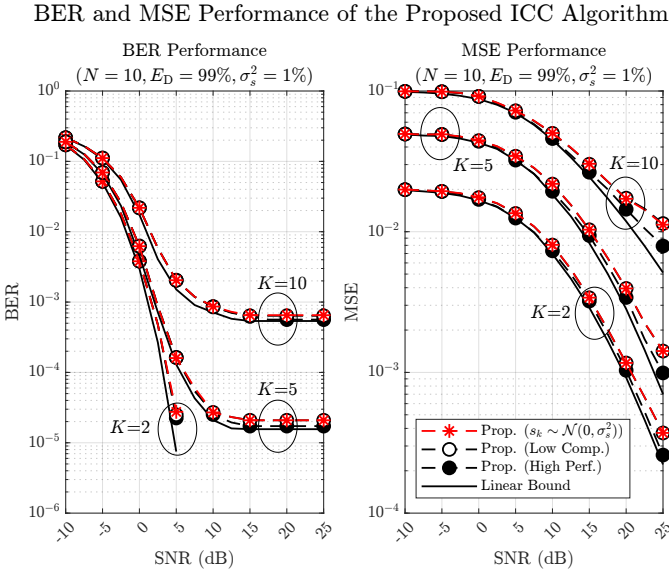


Fig. 2. BER and NMSE performance of the proposed algorithm for the overloaded, underloaded and fully-loaded scenarios.

⁵Notice that as a result of the bivariate estimation carried out, the fully loaded case is actually when $N = 10$ and $K = 5$ since a total of $2K$ variables in the form of data and computing symbols need to be estimated from N factor nodes.

BER and MSE Performance of the Proposed ICC Algorithm

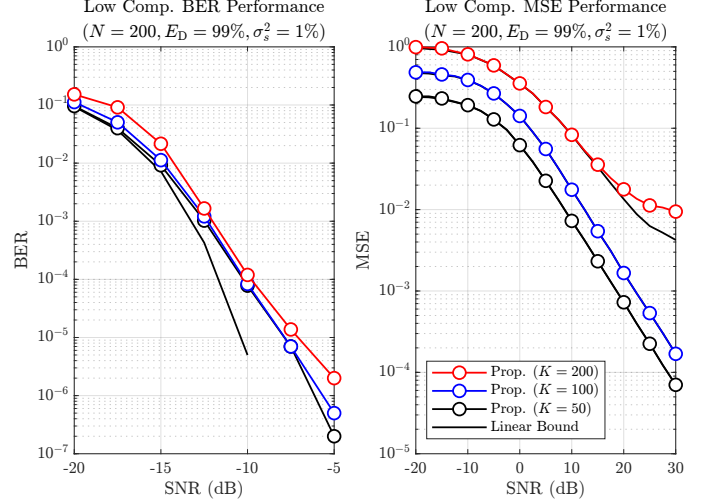


Fig. 3. BER and NMSE Performance of the proposed algorithm in massive systems for the overloaded, underloaded and fully-loaded scenarios.

in Fig. 3 and can also be mitigated via methods such as channel coding and iterative damping [25] for lower system sizes.

Next, we consider a similar system setup but with a much larger number of $N = 200$ antennas servicing a varying number of single-antenna users that are also categorized into the underloaded, fully loaded and overloaded scenarios with $K = 50$, $K = 100$ and $K = 200$ users, respectively, to demonstrate the efficacy of the low complexity variation of the proposed algorithm for enabling ICC in massive scenarios.

As seen in Fig. 3, the BER improves significantly with a larger system which can also be attributed to the strengthening of the SGA utilized in the belief generation stage with the best performance seen by underloaded systems as expected. In addition, considering the MSE performance for computing, we see that the under and fully loaded scenarios reach the appropriate bounds in terms of performance with the overloaded case not too far behind as well, with the distinctions in the variations explained by the increasing variance with a larger K as opposed to the BER results.

B. Complexity Analysis

Since the high performance update requires a matrix inversion of size $N \times N$ at every iteration, the resulting per-iteration computational complexity order is $\mathcal{O}(N^3)$. However, since the low complexity variation only requires this matrix inversion once at the initialization stage, the resulting per-iteration computational complexity order is $\mathcal{O}(NK)$ which is linear on the number of element-wise computations performed.

V. FUTURE/FOLLOW-UP WORK

A. Generalized Nomographic Functions

The following are some distinct nomographic functions whose prior distributions can be exploited for ICC, under the assumption that the individual elements are independent and identically distributed (i.i.d.) and $s_k \sim \mathcal{N}(\mu_s, \sigma_s^2)$.

TABLE I
EXAMPLES OF SOME NOMOGRAPHIC FUNCTIONS AND THEIR PRIORS.

Description	$f(s)$	Prior Distribution
Arithmetic sum	$\sum_{k=1}^K s_k$	$\sim \mathcal{N}(K\mu_s, K\sigma_s^2)$
Arithmetic product	$\prod_{k=1}^K s_k$	[26]
Max operation	$\max_k \{s_k\}$	[27]
Min operation	$\min_k \{s_k\}$	[27]

We also remark that if there exists some non-trivial nomographic function whose prior distributions cannot be computed analytically, they can, for example, be approximated via techniques using Gaussian mixtures or Jacobian methods [28].

B. Multi-stream Computation

Nomographic functions from the same/different streams of signals can also be computed together or separately via the proposed method, provided that there exists some prior distribution with the key advantage being the increase of only one incorporated variable to be estimated in the belief propagation framework.

VI. CONCLUSION

In this manuscript, we proposed a novel framework for the design of practical ICC receivers, with an emphasis on the flexibility and scalability of the systems. Moreover, the resulting receiver framework, which seeks to detect all communication symbols and minimize the distortion over the computing signals, requires that only a fraction of the transmit power be allocated to the latter, therefore coming close to the ideal condition that computing is achieved without sacrificing any communications capability. The key scalability enabler in this case is the utilized GaBP structure relying only on element-wise scalar operations, enabling its use in massive settings, as demonstrated by simulation results incorporating up to 200 antennas and 200 UEs/EDs. Finally, further numerical simulations also demonstrate the efficacy of the proposed method under all various loading conditions, where the performance of the scheme approaches fundamental limiting bounds in under/fully loaded cases with a very low complexity.

REFERENCES

- [1] F. Liu *et al.*, "Integrated Sensing and Communications: Toward Dual-Functional Wireless Networks for 6G and Beyond," *IEEE Journal on Selected Areas in Communications*, vol. 40, no. 6, 2022.
- [2] Q. Qi, X. Chen, C. Zhong, and Z. Zhang, "Integrated Sensing, Computation and Communication in B5G Cellular Internet of Things," *IEEE Trans. Wireless Commun.*, vol. 20, no. 1, 2021.
- [3] C.-X. Wang *et al.*, "On the Road to 6G: Visions, Requirements, Key Technologies, and Testbeds," *IEEE Communications Surveys & Tutorials*, vol. 25, no. 2, 2023.
- [4] K. Shafique *et al.*, "Internet of Things (IoT) for Next-Generation Smart Systems: A Review of Current Challenges, Future Trends and Prospects for Emerging 5G-IoT Scenarios," *IEEE Access*, vol. 8, 2020.
- [5] L. Gaudio, M. Kobayashi, G. Caire, and G. Colavolpe, "On the Effectiveness of OTFS for Joint Radar Parameter Estimation and Communication," *IEEE Trans. Wireless Commun.*, vol. 19, no. 9, 2020.
- [6] K. R. R. Ranasinghe, H. S. Rou, and G. T. F. de Abreu, "Fast and Efficient Sequential Radar Parameter Estimation in MIMO-OTFS Systems," in *IEEE International Conference on Acoustics, Speech and Signal Processing (ICASSP)*, 2024.
- [7] A. Bemani, N. Ksairi, and M. Kountouris, "Integrated Sensing and Communications with Affine Frequency Division Multiplexing," *IEEE Wireless Communications Letters*, 2024.
- [8] K. R. R. Ranasinghe, H. S. Rou, G. T. F. de Abreu, T. Takahashi, and K. Ito, "Joint Channel, Data and Radar Parameter Estimation for AFDM Systems in Doubly-Dispersive Channels," <https://arxiv.org/pdf/2405.16945>, 2024.
- [9] N. González-Prelcic, M. F. Keskin, O. Kaltiokallio, M. Valkama, D. Dardari, X. Shen, Y. Shen, M. Bayraktar, and H. Wymeersch, "The Integrated Sensing and Communication Revolution for 6G: Vision, Techniques, and Applications," *Proceedings of the IEEE*, 2024.
- [10] K. R. R. Ranasinghe, K. Ando, H. S. Rou, G. T. F. de Abreu, and A. Bathelt, "Blind Bistatic Radar Parameter Estimation for AFDM Systems in Doubly-Dispersive Channels," 2024. [Online]. Available: <https://arxiv.org/abs/2407.05328>
- [11] J. Zhang, S. Guo, S. Gong, C. Xing, N. Zhao, D. W. K. Ng, and D. Niyato, "Intelligent Waveform Design for Integrated Sensing and Communication," *IEEE Wireless Communications*, 2024.
- [12] G. Rexhepi, K. R. R. Ranasinghe, G. T. F. de Abreu, and D. G. G., "Tone Reservation-based PAPR Reduction using Manifold Optimization for OFDM-ISAC Systems," 2024. [Online]. Available: <https://arxiv.org/abs/2409.16121>
- [13] B. Nazer and M. Gastpar, "Computation over Multiple-Access Channels," *IEEE Trans. Inf. Theory*, vol. 53, no. 10, 2007.
- [14] W. Liu, X. Zhang, Y. Li, and B. Vucetic, "Over-the-Air Computation Systems: Optimization, Analysis and Scaling Laws," *IEEE Trans. Wireless Commun.*, vol. 19, no. 8, 2020.
- [15] Z. Wang, Y. Zhao, Y. Zhou, Y. Shi, C. Jiang, and K. B. Letaief, "Over-the-Air Computation for 6G: Foundations, Technologies, and Applications," *IEEE Internet of Things Journal*, vol. 11, no. 14, Jul. 2024. [Online]. Available: <http://dx.doi.org/10.1109/JIOT.2024.3405448>
- [16] Q. Lan, H. S. Kang, and K. Huang, "Simultaneous Signal-and-Interference Alignment for Two-Cell Over-the-Air Computation," *IEEE Commun. Lett.*, vol. 9, no. 9, Sep. 2020.
- [17] T. Qin *et al.*, "Over-the-Air Computation via Broadband Channels," *IEEE Wireless Commun. Lett.*, vol. 10, no. 10, 2021.
- [18] L. Chen, X. Qin, and G. Wei, "A Uniform-Forcing Transceiver Design for Over-the-Air Function Computation," *IEEE Wireless Commun. Lett.*, vol. 7, no. 6, 2018.
- [19] W. Fang, Y. Zou, H. Zhu, Y. Shi, and Y. Zhou, "Optimal Receive Beamforming for Over-the-Air Computation," in *IEEE 22nd International Workshop on Signal Processing Advances in Wireless Communications (SPAWC)*, 2021.
- [20] K. Ando and G. T. F. de Abreu, "Low-Complexity and High-Performance Combiners for Over the Air Computing," in *IEEE 9th International Workshop on Computational Advances in Multi-Sensor Adaptive Processing (CAMSAP)*, 2023.
- [21] D. Bickson, "Gaussian Belief Propagation: Theory and Application," 2009.
- [22] B. Li, N. Wu, and Y.-C. Wu, "Distributed Inference With Variational Message Passing in Gaussian Graphical Models: Tradeoffs in Message Schedules and Convergence Conditions," *IEEE Transactions on Signal Processing*, vol. 72, 2024.
- [23] T. Takahashi, S. Ibi, and S. Sampei, "Design of Adaptively Scaled Belief in Multi-Dimensional Signal Detection for Higher-Order Modulation," *IEEE Transactions on Communications*, vol. 67, no. 3, 2019.
- [24] A. Pérez-Neira, M. Martínez-Gost, A. Şahin, S. Razavikia, C. Fischione, and K. Huang, "Waveforms for Computing Over the Air," 2024. [Online]. Available: <https://arxiv.org/abs/2405.17007>
- [25] Q. Su and Y.-C. Wu, "On Convergence Conditions of Gaussian Belief Propagation," *IEEE Trans. on Signal Processing*, vol. 63, no. 5, 2015.
- [26] M. D. Springer and W. E. Thompson, "The Distribution of Products of Independent Random Variables," *SIAM Journal on Applied Mathematics*, vol. 14, no. 3, pp. 511–526, 1966. [Online]. Available: <https://doi.org/10.1137/0114046>
- [27] H. A. David and H. N. Nagaraja, *Order Statistics*. John Wiley & Sons, Ltd, 2006. [Online]. Available: <https://onlinelibrary.wiley.com/doi/abs/10.1002/0471667196.ess6023.pub2>
- [28] G. T. de Abreu, "On the Generation of Tikhonov Variates," *IEEE Transactions on Communications*, vol. 56, no. 7, 2008.